When illusions merge

Aline F. Cretenoud

Laboratory of Psychophysics, Brain Mind Institute, École Polytechnique Fédérale de Lausanne (EPFL), Lausanne, Switzerland ✉

Gregory Francis

Psychological Sciences, Purdue University, West Lafayette, IN, USA ✉

Michael H. Herzog

Laboratory of Psychophysics, Brain Mind Institute, École Polytechnique Fédérale de Lausanne (EPFL), Lausanne, Switzerland ✉

We recently found only weak correlations between the susceptibility to various visual illusions. However, we observed strong correlations among different variants of an illusion, suggesting that the visual space of illusions includes several illusion-specific factors. Here, we specifically examined how factors for the vertical–horizontal, Müller–Lyer, and Ponzo illusions relate to each other. We measured the susceptibility to each illusion separately and to combinations of two illusions, which we refer to as a merged illusion; for example, we tested the Müller–Lyer illusion and the vertical–horizontal illusion, as well as a merged version of both illusions. We used an adjustment procedure in two experiments with 306 and 98 participants, respectively. Using path analyses, correlations, and exploratory factor analyses, we found that the susceptibility to a merged illusion is well predicted from the susceptibilities to the individual illusions. We suggest that there are illusion-specific factors that, by independent combinations, represent the whole visual structure underlying illusions.

Introduction

Common factors are frequently encountered in everyday life. For example, the Big Five personality traits scale determines five different aspects of personality: openness to experience, conscientiousness, extraversion, agreeableness, and neuroticism (John & Srivastava, 1999). These five specific factors are supposed to represent the factor structure of personality. Similarly, *g* (general intelligence) is a common factor for intelligence that can be inferred from several specific factors, such as the Wechsler scale (Wechsler, 2003). Likewise, touch and audition have been shown to correlate highly, reflecting a common factor for somatosensation (Frenzel et al., 2012).

For vision, however, there seems to be no strong, unique factor but rather several specific ones (for reviews, see Mollon, Bosten, Peterzell, & Webster, 2017; Peterzell, 2016; Tulver, 2019). For example, more than 1000 participants were tested with 25 visual and auditory measures (Bosten, Goodbourn, Bargary, Verhallen, Lawrance-Owen, Hogg, & Mollon, 2017). Only 20% of the total variance underlying these 25 measures was explained by a unique factor, whereas eight specific factors explained about 57% of the total variance. In addition, Brascamp, Becker, and Hambrick (2018) claimed that there is only weak evidence for a single mechanism (i.e., a common factor) to underlie different forms of bistable perception, such as binocular rivalry (see also Cao, Wang, Sun, Engel, & He, 2018). Similarly, there was only weak evidence for a unique factor in contrast perception (Bosten & Mollon, 2010; Peterzell, 2016; Peterzell, Schefrin, Tregear, & Werner, 2000), eye movements (Bargary, Bosten, Goodbourn, Lawrance-Owen, Hogg, & Mollon, 2017), face recognition (Verhallen, Bosten, Goodbourn, Lawrance-Owen, Bargary, & Mollon, 2017), hue scaling (e.g., Emery, Volbrecht, Peterzell, & Webster, 2017a; Emery, Volbrecht, Peterzell, & Webster, 2017b), local–global processing (Chamberlain, Van der Hallen, Huygelier, Van de Cruys, & Wagemans, 2017; Milne & Szczerbinski, 2009), color matching (Webster & MacLeod, 1988), stereopsis (e.g., Hibbard, Bradshaw, Langley, & Rogers, 2002; Peterzell, Serrano-Pedraza, Widdall, & Read, 2017), luminance contrast sensitivity (Dobkins, Gunther, & Peterzell, 2000; Peterzell, Chang, & Teller, 2000), and in the use of expectations and knowledge priors (Tulver, Aru, Rutiku, & Bachmann, 2019), suggesting that the structure of visual space is multifactorial. Only weak correlations were also found between performance in six basic visual tasks,

such as visual backward masking and Vernier offset discrimination (Cappe, Clarke, Mohr, & Herzog, 2014).

Likewise, only weak correlations were observed between the susceptibility to different illusions, such as the Ebbinghaus and Müller–Lyer illusions (Grzeczkowski, Clarke, Francis, Mast, & Herzog, 2017; Grzeczkowski, Roinishvili, Chkonia, Brand, Mast, Herzog, & Shaqiri, 2018), suggesting that the structure of the visual space underlying illusions is multifactorial. Factors specific to classes of illusions have been found in the past. For example, Thurstone (1944) found a factor underlying geometric illusions that, however, did not show strong loadings on other classes of illusions such as brightness or size–weight illusions. Likewise, Coren, Girgus, Erlichman, and Hakstian (1976) suggested that visual illusions can be classified into two classes: illusions of linear extent and illusions of shape or direction (see also Robinson, 1968). Taylor (1974, 1976) found that a set of different illusion measures was best represented by a three- or four-factor model, suggesting that visual illusions are heterogeneous perceptual tasks (but see Aftanas & Royce, 1969; Roff, 1953). Similarly, it has recently been suggested (Bulatov, 2017) that the visual structure underlying illusions of spatial extent, such as the Müller–Lyer illusion, combines several physiological and psychological factors.

Recently, we tested several variants of the Ebbinghaus illusion, differing in color, shape, size, and texture, and found strong correlations between the susceptibility to all variants. Similarly, when testing several illusions with different luminance, orientation, and contextual conditions, strong within-illusion correlations but only weak between-illusion correlations were observed (Cretenoud, Grzeczkowski, Bertamini, & Herzog, 2020; Cretenoud, Karimpur, Grzeczkowski, Francis, Hamburger, & Herzog, 2019); that is, an individual who is strongly susceptible to one illusion is not necessarily strongly susceptible to a different illusion, but there is a high probability for this individual to also be strongly susceptible to another variant of the same illusion. We suggested that factors are illusion-specific, even though a small proportion of the variance in the illusion magnitudes (especially in some subsets of illusions) may be accounted for by a general—but weak—common factor.

Here, we wondered how these factors relate to each other. To this aim, we merged pairs of illusions and tested whether the susceptibility to a merged illusion can be predicted from the susceptibilities to the non-merged illusions of which it was made.

Experiment 1

Methods

Participants

Participants were students at Purdue University who received course credit in return for their participation.

Among the 310 students that took part in this experiment, 306 were considered for further analysis (four participants were considered as outliers). Ages ranged from 19 to 27 years (mean age, 22 years), and 109 females participated. Two participants did not provide any information about their gender. Procedures were conducted in accordance with the tenets of the Declaration of Helsinki, except for the preregistration, and were approved by the local ethics committee.

Apparatus

Each participant ran the experiment on their own computer in a web browser over the Internet. Due to the online nature of the experiment, the details of a participant's computer and screen are mostly unknown. The experiment software was able to verify that the web browser was on a desktop or laptop computer rather than on a handheld device. Participants trying to access the experiment with a phone or tablet were asked to try again with a desktop or laptop computer.

Stimuli

Figure 1 provides a schematic of the stimuli used in Experiment 1. A horizontal reference line on the bottom right was either 100 or 150 pixels long. An adjustable line on the top left had a length randomly selected between 15 pixels and an upper limit that was itself randomly chosen to be 75 to 100 pixels larger than the length of the reference line, with the restriction that it could not be closer than 15 pixels to the length of the reference line. Each line was 2 pixels thick. The adjustable line was presented either horizontally or vertically, as in the vertical–horizontal illusion. As in the Müller–Lyer illusion, inward and outward wings were added to some conditions in a virtual square with sides of 15 pixels and at a 45° angle relative to the adjustable line. With two reference line lengths (100 and 150 pixels), two adjustable line orientations (horizontal and vertical), and three types of wings (inward, none, and outward) for the adjustable line, there were 12 stimulus conditions.

Because the reference line was always horizontal, we considered the adjustable line in the horizontal no wings conditions (HorNone100 and HorNone150) to be control conditions. In addition to these control conditions, we considered six conditions as non-merged conditions because they referred to one illusory effect only: a vertical–horizontal illusion in which the vertical line is usually perceived as being longer than a horizontal line of the same length (vertical no wings conditions: VerNone100 and VerNone150) or a Müller–Lyer illusion in which a line with inward wings usually looks shorter than the same line with outward wings (horizontal inward wings conditions: HorIn100 and HorIn150; horizontal outward wings conditions: HorOut100 and HorOut150). Four conditions were considered as merged conditions because they included
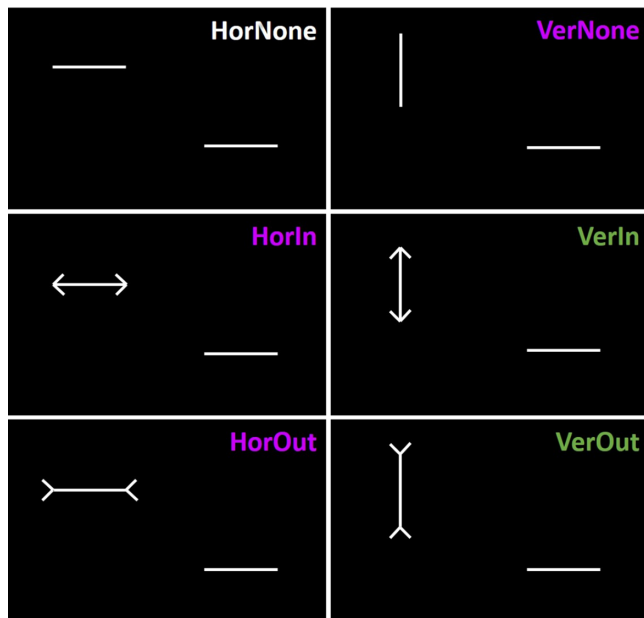
Figure 1. In Experiment 1, 12 conditions were tested. The six conditions illustrated here (2 adjustable line orientations × 3 types of wings) were tested with two reference line lengths (100 and 150 pixels). Abbreviations: "Hor" = horizontal adjustable line; "Ver" = vertical adjustable line; "None"= no wings; "In" = inward wings; "Out" = outward wings. The participant moved a slider to adjust the length of the top left line so that it appeared to be same length as the reference line on the bottom right. Conditions with purple labels show non-merged conditions, as they refer to one illusory effect only (either vertical–horizontal or Müller–Lyer illusion), whereas conditions with green labels show merged conditions. We considered the comparison of two horizontal lines (HorNone conditions; white label) as purely non-illusory.

both illusory effects: the adjustable line was a vertical line with either inward wings (VerIn100 and VerIn150) or outward wings (VerOut100 and VerOut150).

Procedure

Each trial started when the participant clicked a button. A condition appeared on the screen and the participant moved a slider to the left or right to change the length of the adjustable line. The task was to set the length of the adjustable line so that it appeared to be the same length as the reference line. When the participants were satisfied that the lines looked the same length, they clicked on a "Submit Match" button to end the trial. The first four trials were practice trials that presented all combinations of reference line length and adjustable line orientation. The adjustable line always had no wings during the practice trials. For subsequent trials, each condition was presented eight times in a random order. The final three questions gathered demographic

information (sex, age, and ethnicity). The experiment took less than 30 minutes to complete.

Data analysis

Intrarater reliability was assessed by computing two-way mixed-effects models (intraclass correlations of type [3,1] or $ICC_{3,1}$) for each condition, as suggested in Shrout and Fleiss (1979) and in Koo and Li (2016).

The eight adjustments of each participant were averaged for each condition. To compute illusion strength, the reference line length (either 100 or 150 pixels) was subtracted from the mean adjustments. The results were subsequently divided by the same reference line length, thus turning them into illusion magnitudes as a proportion of the reference line length. Overadjustments and underadjustments are indicated by positive and negative illusion magnitudes, respectively. Analyses were performed in R (R Core Team, 2018).

To check for outliers, illusion magnitudes were standardized. Rather than the commonly used z-scores, we used modified z-scores, which are based on the median and the median absolute deviation (Iglewicz & Hoaglin, 1993). Modified z-scores were summed (in absolute values) for each participant across all conditions. Four participants were considered as outliers and removed from the dataset because the sum of their modified z-scores was outside the mean ± 3 standard deviations (*SD*s) range.

A three-way repeated measures analysis of variance (ANOVA) was performed on the illusion magnitudes after outlier removal. We used Mauchly's tests to verify sphericity assumptions and applied Greenhouse–Geisser correction in case of violations of sphericity. In both experiments, the alpha level for statistical significance was set to 0.05.

To determine whether merged illusion magnitudes can be predicted from non-merged illusion magnitudes, a path analysis was computed with the vertical inward wings and vertical outward wings conditions as outcomes (VerIn100, VerIn150, VerOut100, and VerOut150; endogenous variables) and all the other conditions as predictors (exogenous variables). In a path analysis, each predictor is regressed onto each outcome (Beaujean, 2014). The vertical inward wings (VerIn) conditions were expected to be strongly predicted from the vertical no wings (VerNone) and horizontal inward wings (HorIn) conditions. Likewise, we expected the vertical no wings (VerNone) and horizontal outward wings (HorOut) conditions to strongly predict the vertical outward wings (VerOut) conditions. Importantly, the path model considers the covariances among the exogenous variables (i.e., control and non-merged conditions).

We computed Pearson's correlations between the illusion magnitudes of each condition and participants'

Test	F	df_1	df_2	η_p^2
Orientation	197.687[***]	1	305	0.393
Reference length	1431.100[***]	1	305	0.824
Wings	2023.802[***]	1.997	608.971	0.869
Orientation × reference length	0.267	1	305	<0.001
Orientation × wings	217.404[***]	1.974	601.993	0.416
Reference length × wings	7.435[***]	1.992	607.428	0.024
Orientation × reference length × wings	0.528	1.950	594.645	0.002

Table 1. Statistical results from the three-way repeated measures ANOVA for illusion magnitudes in Experiment 1 with adjustable line orientation, reference line length, and type of wings as main factors. [***]$p < 0.001$

age. We found no significant effects (see Table S1A in the Supplementary Material). We also computed Pearson's correlations between the illusion magnitudes of each pair of conditions. Finally, an exploratory factor analysis (EFA) was computed to explore the factors underlying the global structure of the dataset using the guidelines outlined in Preacher, Zhang, Kim, and Mels (2013). Because our aim was to identify factors reflecting only the variance shared between conditions (i.e., the common variance), we extracted factors with a common factor analysis. An oblique rotation (promax) was used in the EFA because we had no reason to preclude factors to correlate. Similar loadings are observed with an oblique or orthogonal rotation if the factors are uncorrelated (e.g., Costello & Osborne, 2005). We should mention that an EFA explores the structure underlying a dataset (i.e., the EFA looks for latent factors), whereas a path analysis explores the linear relationships between measured variables.

Results

Intrarater reliability

All conditions showed significant intraclass correlations even after Bonferroni correction was applied, highlighting consistent adjustments across all eight trials of the same condition (Table 2B, diagonal). We should note, however, that the correlation coefficients indicate a large range of reliabilities from poor (HorNone100 ICC coefficient = 0.119) to large (VerIn150 ICC coefficient = 0.329) according to Gignac and Szodorai (2016) but only poor to moderate according to Cohen (1988).

Magnitudes of the illusions

The illusion magnitudes are illustrated in Figure 2 and summarized in the Supplementary Material (Table S2A). A three-way repeated measures ANOVA was computed with the main factors of adjustable line orientation (horizontal or vertical), reference line length
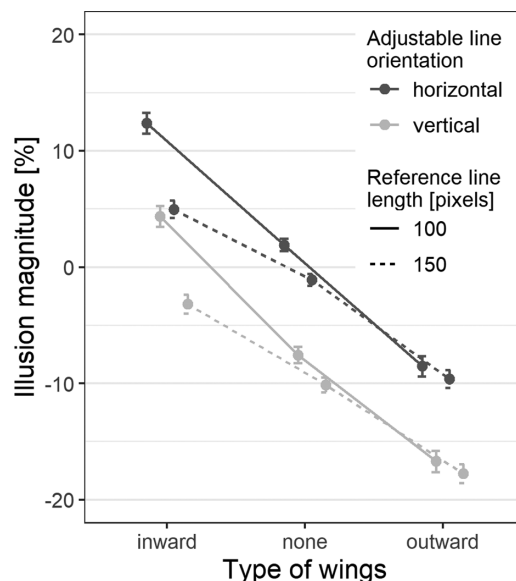

Figure 2. Illusion magnitudes $\pm$ 2 *SEM* in Experiment 1 as a function of the type of wings (inward, none, or outward), the adjustable line orientation (dark gray, horizontal; light gray, vertical), and the reference line length (solid line, 100 pixels; dotted line, 150 pixels). Positive and negative magnitudes indicate overadjustments and underadjustments compared to the reference, respectively.

(100 or 150 pixels), and type of wings (inward, none, or outward). Statistical results are shown in Table 1.

Path analysis

A path analysis was computed to determine whether the illusion magnitudes of the merged conditions can be predicted from the illusion magnitudes of the two non-merged conditions of which it was made. Standardized path coefficients are reported in Table 2A. The two non-merged conditions that made each merged condition (i.e., the expected predictors) showed significant path coefficients. A Welch two-tailed *t*-test between the path coefficients that were expected to be high ($M = 0.317$, $SD = 0.100$) and the others ($M = 0.049$, $SD = 0.115$) resulted in a significant difference

(A)	HorNone100	HorNone150	HorIn100	HorIn150	HorOut100	HorOut150	VerNone100	VerNone150	r^2
VerIn100	-.044	-.050	.495***	.020	.069	.028	.212***	.200***	.513
VerIn150	-.072	.052	.271***	.253***	-.114*	.164**	.122*	.308***	.544
VerOut100	.054	-.110*	.176**	-.198***	.387***	.212***	.196***	.139**	.548
VerOut150	.001	-.038	.053	.068	.087	.306***	.096	.378***	.488

(B)	HorNone100	HorNone150	HorIn100	HorIn150	HorOut100	HorOut150	VerNone100	VerNone150	VerIn100	VerIn150	VerOut100	VerOut150
HorNone100	.119	.372	.380	.205	.374	.255	.437	.231	.302	.226	.356	.261
HorNone150		.171	.226	.461	.113	.446	.123	.423	.186	.408	.080	.324
HorIn100			.238	.484	.508	.429	.347	.172	.632	.485	.456	.352
HorIn150				.253	.221	.550	.023	.365	.336	.573	.105	.405
HorOut100					.194	.442	.413	.197	.442	.242	.643	.375
HorOut150						.230	.165	.396	.363	.516	.402	.554
VerNone100							.177	.417	.476	.305	.516	.356
VerNone150								.274	.374	.546	.305	.575
VerIn100									.277	.627	.523	.491
VerIn150										.329	.369	.635
VerOut100											.270	.584
VerOut150												.324

Table 2. Experiment 1. (A) Standardized path coefficients ($^*p < 0.05$, $^{**}p < 0.01$, $^{***}p < 0.001$) from the path analysis and communalities (i.e., the variance explained, r^2) of each merged condition. Gray shading indicates the non-merged conditions that made up every merged condition (i.e., expected predictors). (B) Diagonal (in gray): Intrarater reliabilities expressed as intraclass correlation coefficients ($ICC_{3,1}$) for each condition. All of them were significant. Triangle: Correlations between each pair of conditions expressed as correlation coefficients (Pearson's r). A color scale from white to red reflects effect sizes from $r = 0$ to $r = 1$ (no negative effect sizes). Italics and bold font indicate significant results without and with Bonferroni correction, respectively. Black labels indicate control (non-illusory) conditions; purple labels indicate non-merged conditions; green labels indicate merged conditions

($t[13.668] = 6.298$, $p < 0.001$, $d = 2.483$). However, some unexpected, non-merged conditions significantly loaded on the merged conditions. For example, not only the VerNone100 and HorIn100 conditions significantly loaded on the VerIn100 condition (standardized path coefficients: VerNone100 = 0.212, $p < 0.001$; HorIn100 = 0.495, $p < 0.001$), but also the VerNone150 condition (standardized path coefficient = 0.200, $p < 0.001$). However, this might be due to the very strong correlations observed between conditions, especially between the two reference line lengths of a same combination of adjustable line orientation and type of wings.

We observed only weak path coefficients from the horizontal no wings conditions (HorNone100 and HorNone150) to the merged conditions, which was expected as these two conditions were considered to be control conditions. Indeed, the adjustable line was presented horizontally (unlike the vertical–horizontal illusion) and with no additional wings (unlike the Müller–Lyer illusion) in both control conditions. Table 2A also shows the communalities of each merged condition (i.e., the variance explained, or r^2). The uniqueness (i.e., the variance not explained by the exogenous variables, or $1 - r^2$) of each merged condition was between 0.452 and 0.512.

	RF1	RF2
HorNone100	0.427	0.099
HorNone150	−0.175	0.696
HorIn100	0.484	0.252
HorIn150	−0.231	0.889
HorOut100	0.759	−0.096
HorOut150	0.134	0.622
VerNone100	0.735	−0.146
VerNone150	0.134	0.523
VerIn100	0.584	0.215
VerIn150	0.120	0.732
VerOut100	0.948	−0.190
VerOut150	0.356	0.471

Table 3. Rotated factor loadings from an EFA after promax rotation for all conditions of Experiment 1. A color scale from blue (negative loadings) to red (positive loadings) is shown. Black indicates control (non-illusory) conditions; purple indicates non-merged conditions; green indicates merged conditions. The two factors seem to relate to the two reference line length conditions

Correlations

Correlations between the illusion magnitudes of each pair of conditions are reported in Table 2B (triangle). Interestingly, most correlations were significant even after Bonferroni correction was applied for multiple comparisons. The effect sizes of the eight between-illusion correlations—correlations between a condition that refers to the vertical–horizontal illusion only (VerNone conditions) and a condition that refers to the Müller–Lyer illusion only (HorIn and HorOut conditions)—were significantly different from zero (one-sample two-tailed t-test: $t[7] = 5.244$, $p = 0.001$, $d = 1.854$).

Exploratory factor analysis

A two-factor model was suggested by a scree plot inspection (see Figure S1A in the Supplementary Material), whereas a parallel analysis suggested a five-factor model. Because the eigenvalues of factors three to five were well below one (RF1, 4.645; RF2, 0.996; RF3, 0.448; RF4, 0.309; RF5, 0.245), we retained the two-factor model. Loadings from the two-factor model are reported in Table 3. The two factors together explained 49% of the variance (RF1, 25%; RF2, 24%). They were strongly inter-correlated ($r = 0.597$) and seem to relate to the two reference line length conditions.

Experiment 2

Methods

Participants

Participants were 100 visitors at a public event organized in Geneva, Switzerland. Of these, 98 participants were considered for further analysis (there were two outliers), with age ranging from 8 to 81 years (mean age, 36 years; 57 females). Adults signed informed consent and we obtained the assent of children as well as the consent of their parents. Participation was not compensated for in any form. Procedures were conducted in accordance with the tenets of the Declaration of Helsinki, except for the preregistration, and were approved by the local ethics committee.

Apparatus

The experiment was coded in MATLAB (R2014b, 64 bits; MathWorks, Natick, MA) using the Psychophysics Toolbox 3.1 (64 bits; Brainard, 1997; Pelli, 1997) and was presented on a 24.5-inch BenQ monitor (Taipei, Taiwan) at a resolution of 1920 × 1080 pixels with a 60-Hz refresh rate. Participants sat approximately 60 cm away from the screen and used a Logitech LS1 computer mouse (Lausanne, Switzerland) to fulfill the task. A Minolta LS-100 luminance meter (Osaka, Japan) was used to calibrate the monitor before the experiment began. A room with artificial light conditions was used to run the experiment.

Stimuli

Stimuli were presented in white ($\sim$176 cd/m^2) on a black background ($\sim$1 cd/m^2). The line width was 4 pixels. Participants were tested with the vertical–horizontal (VH), Müller–Lyer (ML), and Ponzo (PZ) illusions (Figure 3). In addition, the vertical–horizontal and Müller–Lyer illusions were congruently (VH-ML con.) and incongruently (VH-ML inc.) merged. In the congruent VH-ML illusion, inward and outward wings were added to the horizontal and vertical segments of the vertical–horizontal illusion, respectively. In the incongruent VH-ML illusion, inward and outward wings were drawn at the extremities of the vertical and horizontal segments of the vertical–horizontal illusion, respectively. Similarly, the Müller–Lyer and Ponzo illusions were congruently merged (PZ-ML con.) by adding inward and outward wings to the lower and upper horizontal segments of the Ponzo illusion, respectively, and incongruently merged (PZ-ML inc.) when the contrary was true. In total, seven illusions were tested.
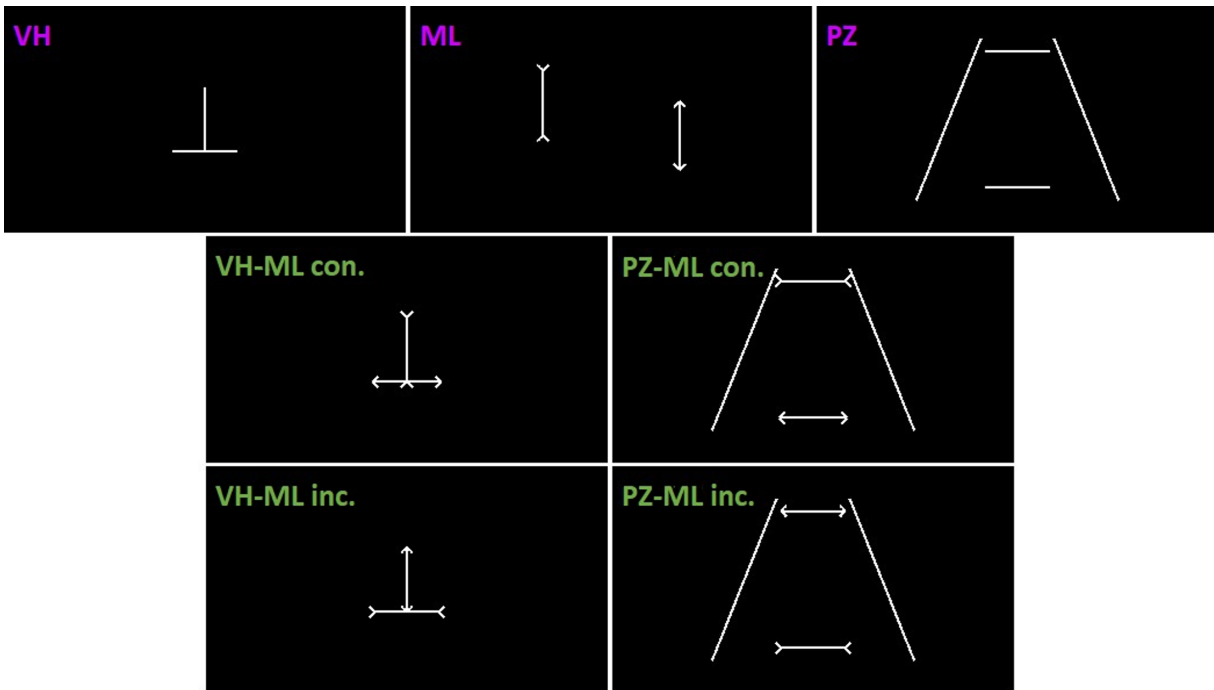
Figure 3. Seven illusions were tested in Experiment 2 with an adjustment procedure: the vertical-horizontal (VH), Müller–Lyer (ML) and Ponzo (PZ) illusions, as well as the vertical–horizontal illusion congruently merged (VH-ML con.) or incongruently merged (VH-ML inc.) with the Müller–Lyer illusion and the Ponzo illusion congruently merged (PZ-ML con.) or incongruently merged (PZ-ML inc.) with the Müller–Lyer illusion. Two configurations were tested for each illusion (e.g., either the horizontal or vertical segment of the VH illusion was adjusted), making up 14 conditions. There were two trials of each condition. Purple indicates non-merged illusions; green indicates merged illusions.

In the VH and the congruent and incongruent VH-ML illusions, participants were asked to adjust the length of the horizontal segment to match the length of the vertical segment or to adjust the length of the vertical segment to match the length of the horizontal segment. In the ML illusion, we asked participants to adjust the length of the segment with inward wings to match the length of the segment with outward wings, and vice versa. In the PZ and the congruent and incongruent PZ-ML illusions, the task was to adjust the upper segment in length to match the lower one in length, and vice versa. Hence, each illusion was tested under two configurations, as one segment was in turn the reference or the adjustable segment. Adjustments were made by moving the computer mouse, and participants validated their adjustments by clicking on the left button of the computer mouse.

In each illusion, the reference segment was 8° long, and the length of the adjustable segment was pseudorandomly chosen to be between 2° and 14° at the beginning of each trial. In the ML, congruent and incongruent VH-ML, and congruent and incongruent PZ-ML illusions, the wings were 1° long and rotated by 45° compared to the orientation of the segments. In the VH and the congruent and incongruent VH-ML illusions, the center of the horizontal segment was

displayed 4° to the bottom of the midscreen, and the vertical segment was always touching it. In the ML illusion, the distance between the two segments was 16.9°. The centers of the segments with outward and inward wings were presented 2° to the top and bottom of the midscreen, respectively. In the PZ and the congruent and incongruent PZ-ML illusions, the two segments were 16.9° apart from each other. The distances between the upper and lower ends of the diagonals were 9° and 25°, respectively, and the total height of the illusion was 20°.

Procedure

The experimenter first explained the task to the participants. Three practice trials were run in order to ensure that the participants correctly understood the task: one ML trial, one VH-ML trial (either congruent or incongruent), and one PZ-ML trial (either congruent or incongruent). Each condition (7 illusions × 2 configurations = 14 conditions) was tested twice, resulting in 28 trials per participant. The order of presentation of the 28 trials was chosen randomly by the computer. Participants were asked to refrain from any prior knowledge about visual illusions and to rely on their percepts only. The experimenter stayed
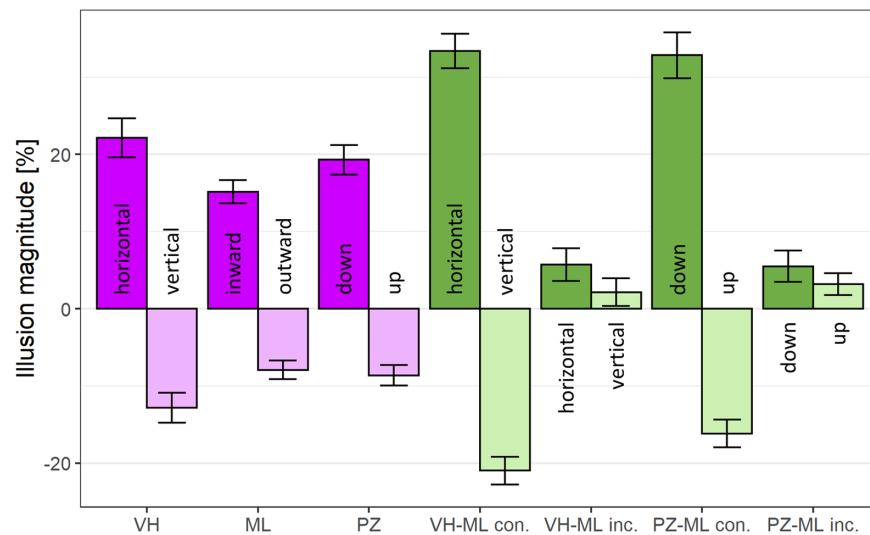
Figure 4. Illusion magnitudes $\pm$ 2 *SEM* in Experiment 2. Purple indicates non-merged conditions; green indicates merged conditions.

in the room during the experiment and answered any questions at any time. At the end of the experiment, the participants were shown their results and debriefed.

Data analysis

Intrarater reliability was assessed by computing intraclass correlations, as in Experiment 1. For each participant and each condition, the adjustments from both trials were averaged. As in Experiment 1, illusion magnitudes were computed. In order to make the magnitudes comparable across illusions, modified *z*-scores were computed for each illusion. At this stage, two outliers were detected and removed from the dataset. A path analysis was computed to determine whether the illusion magnitudes of the merged conditions (VH-ML con. hor., VH-ML con. ver., VH-ML inc. hor., VH-ML inc. ver., PZ-ML con. down, PZ-ML con. up, PZ-ML inc. down, and PZ-ML inc. up) can be predicted from the illusion magnitudes of the non-merged conditions (VH hor., VH ver., ML in., ML out., PZ down, and PZ up). As in Experiment 1, age did not significantly influence illusion magnitudes (see Table S1B in the Supplementary Material). Finally, we computed pairwise correlations and an EFA as in Experiment 1.

Results

Intrarater reliability

All intraclass correlations were significant even after Bonferroni correction was applied (Table 4B, diagonal).

Magnitudes of the illusions

As expected, all non-merged illusions showed an over-adjusted and an underadjusted configuration (Figure 4 and see Table S2B in the Supplementary Material). For example, the horizontal segment of the vertical–horizontal illusion in which both segments are the same length is usually perceived to be shorter than the vertical segment and was therefore overadjusted (VH hor.: $M = 22.152\%$; $SEM = 1.266\%$). The vertical segment of the same illusion was underadjusted (VH ver.: $M = -12.829\%$; $SEM = 0.979\%$) because it is usually perceived to be longer than the horizontal segment. Interestingly, however, the illusion magnitudes are not symmetrical across both configurations. For example, the PZ down condition showed stronger absolute illusion magnitude compared to the PZ up condition (PZ down: $M = 19.301\%$, $SEM = 0.966\%$; PZ up: $M = -8.646\%$, $SEM = 0.661\%$). Stronger illusion magnitudes were observed for congruently merged illusions compared to non-merged illusions, while incongruently merged illusions revealed only very weak effects.

Path analysis

We conducted a path analysis with the non-merged conditions as predictors and observed that the illusion magnitude of a merged condition was strongly predicted by the illusion magnitudes of the non-merged conditions of which it was made (Table 4A). For example, adjusting the vertical segment of the incongruent VH-ML illusion (VH-ML inc. ver.) referred to both the vertical VH (VH ver.) and the inward ML (ML in.) conditions. Both the vertical VH (VH ver.) and the inward ML (ML in.) conditions

(A)	VH hor.	VH ver.	ML in.	ML out.	PZ down	PZ up	r^2
VH-ML con. hor.	.601***	−.113	.175*	.110	−.069	−.151	.452
VH-ML con. ver.	−.122	.606***	.053	.301***	.004	.024	.524
VH-ML inc. hor.	.606***	.037	.122	.093	.073	.050	.455
VH-ML inc. ver.	−.022	.530***	.194*	.100	−.105	.016	.341
PZ-ML con. down	.194*	−.029	.165*	.120	.451***	−.177	.437
PZ-ML con. up	−.003	.083	.119	.260**	−.221*	.484***	.446
PZ-ML inc. down	.235*	.143	−.037	.332***	.328***	−.166	.389
PZ-ML inc. up	.080	−.092	.104	−.008	−.079	.391***	.233

(B)	VH hor.	VH ver.	ML in.	ML out.	PZ down	PZ up	VH-ML con. hor.	VH-ML con. ver.	VH-ML inc. hor.	VH-ML inc. ver.	PZ-ML con. down	PZ-ML con. up	PZ-ML inc. down	PZ-ML inc. up
VH hor.	.496	−.360	.111	.158	.184	.285	.622	−.279	.649	−.191	.274	.118	.245	.220
VH ver.		.317	−.044	.032	−.046	.000	−.330	.656	−.187	.538	−.123	.098	.056	−.121
ML in.			.394	.017	.146	.074	.227	.020	.204	.156	.243	.123	.024	.135
ML out.				.311	.148	.045	.188	.304	.205	.102	.211	.253	.414	.010
PZ down					.647	−.359	.143	−.002	.196	−.096	.594	−.343	.468	−.186
PZ up						.428	.063	.005	.210	.066	−.266	.583	−.204	.450
VH-ML con. hor.							.311	-.283	.549	−.183	.399	.000	.130	.264
VH-ML con. ver.								.529	−.181	.576	−.131	.280	.221	−.256
VH-ML inc. hor.									.343	−.082	.297	.061	.247	.242
VH-ML inc. ver.										.297	−.015	.072	−.060	.006
PZ-ML con. down											.574	−.388	.364	.142
PZ-ML con. up												.486	.096	.097
PZ-ML inc. down													.623	−.320
PZ-ML inc. up														.501

Table 4. Experiment 2. (A) Standardized path coefficients (*$p < 0.05$, **$p < 0.01$, ***$p < 0.001$) from the path analysis and communalities (i.e., the variance explained, r^2) of each merged condition. Gray shading indicates the non-merged conditions that made up every merged condition (i.e., expected predictors). (B) Diagonal (in gray): Intrarater reliabilities expressed as intraclass correlation coefficients ($ICC_{3,1}$) for each condition. All of them were significant. Triangle: Correlations between each pair of conditions expressed as correlation coefficients (Pearson's r). A color scale from blue to red reflects effect sizes from $r = -1$ to $r = 1$ (white corresponds to $r = 0$). Italics and bold font indicate significant results without and with Bonferroni correction, respectively. Purple labels indicate non-merged conditions; green labels indicate merged conditions

showed significant standardized path coefficients (VH ver.: 0.530, $p < 0.001$; ML in.: 0.194, $p = 0.021$) to the vertical incongruent VH-ML condition (VH-ML inc. ver.). A Welch two-tailed t-test between the path coefficients that were expected to be high ($M = 0.351$, $SD = 0.180$) and the others ($M = 0.005$, $SD = 0.113$) resulted in a significant difference ($t[21.127] = 7.045$, $p < 0.001$, $d = 2.307$). The communalities of

each merged condition are reported in Table 4A. The uniqueness of each merged condition was between 0.476 and 0.767.

Correlations

Correlations were computed between the illusion magnitudes of each pair of conditions (Table 4B,

triangle). Only three correlations were significant between the two configurations of the same illusion (significant with Bonferroni correction for VH: $r =$ –0.360, $p < 0.001$; PZ: $r =$ –0.359, $p < 0.001$; PZ-ML con.: $r =$ –0.388, $p < 0.001$).

Significant correlations were observed between some merged conditions and the non-merged conditions of which they were made. For example, the horizontal congruent and incongruent VH-ML conditions (VH-ML con. hor. and VH-ML inc. hor.) significantly correlated with the horizontal VH condition (VH hor.). Interestingly, only weak correlations were observed between the merged conditions and the Müller–Lyer illusion (ML in. and ML out. conditions). Hence, when two illusions merge, one illusion seems stronger than the other. This was also observed from the path analysis (Table 4A), where path coefficients to the merged conditions are weaker from the Müller–Lyer conditions than from the vertical–horizontal or Ponzo conditions.

A one-sample two-tailed *t*-test on the effect sizes of the 28 between-illusion correlations (VH vs. ML conditions, VH vs. PZ conditions, ML vs. PZ conditions, VH vs. PZ-ML conditions, and PZ vs. VH-ML conditions) was significantly different from zero ($t[27] = 4.029$, $p < 0.001$, $d = 0.761$), suggesting that a small proportion of the variance underlying the VH, ML, and PZ illusions is accounted for by a weak common factor.

Exploratory factor analysis

As in Experiment 1, a common factor analysis was computed to extract factors. A parallel analysis and scree plot inspection (see Figure S1B in the Supplementary Material) suggested a four-factor model explaining 56% of the total variance (RF1, 16%; RF2, 14%; RF3, 14%; RF4, 12%). The first and third factors highly loaded on the different conditions including the horizontal and vertical configurations of the VH illusion, respectively, whereas the second and forth factors highly loaded on the conditions including the PZ and ML illusions, respectively (Table 5). The interfactor correlations showed small to medium effect sizes (RF1–RF2, $r = 0.024$; RF1–RF3, $r = -0.166$; RF1–RF4, $r = 0.164$; RF2–RF3, $r = 0.098$; RF2–RF4, $r = -0.203$; RF3–RF4, $r = 0.068$).

Discussion

We previously found strong correlations between variants of one illusion but weak correlations between different illusions (Cretenoud et al., 2019; Cretenoud et al., 2020; Grzeczkowski et al., 2017; Grzeczkowski et al., 2018), arguing for a multitude of factors

	RF1	RF2	RF3	RF4
VH hor.	**0.628**	0.158	–0.308	0.226
VH ver.	–0.150	0.009	**0.699**	0.048
ML in.	0.353	–0.054	0.157	**–0.032**
ML out.	0.182	0.131	0.141	**0.460**
PZ down	0.181	**–0.542**	0.000	0.340
PZ up	0.337	**0.692**	0.046	–0.119
VH-ML con. hor.	**0.651**	–0.041	–0.218	**0.076**
VH-ML con. ver.	–0.171	0.153	**0.770**	**0.366**
VH-ML inc. hor.	**0.649**	0.066	–0.120	**0.183**
VH-ML inc. ver.	0.131	–0.024	**0.774**	**–0.106**
PZ-ML con. down	0.547	**–0.621**	0.090	**0.106**
PZ-ML con. up	0.021	**0.831**	0.064	**0.330**
PZ-ML inc. down	0.008	–0.073	–0.037	**0.856**
PZ-ML inc. up	0.550	**0.152**	0.038	**–0.422**

Table 5. Rotated factor loadings from an EFA after promax rotation for all conditions of Experiment 2. A color scale from blue (negative loadings) to red (positive loadings) is shown. Purple indicates non-merged conditions; green indicates merged conditions. Bold numbers indicate loadings that are expected to be high under the hypothesis that the factors relate to conditions including horizontal VH, PZ, vertical VH, and ML, respectively

underlying illusions. Here, we investigated how these factors interact. To this aim, we merged two illusions.

Our results suggest that there are many illusion-specific factors that combine through combinatorics. Indeed, the results from the path analyses suggest that the illusion magnitudes of the merged conditions can be predicted from the illusion magnitudes of the non-merged conditions of which they were made. Our results support the hypothesis that the factors underlying visual illusions combine independently, which is well captured by the linear regressions of the path analyses. However, we have not tested for nonlinear models.

In Experiment 1, we expected to find two factors, one related to the Müller–Lyer and the other related to the vertical–horizontal illusion. We indeed observed two factors, but they seem to relate to the reference line lengths (i.e., the 100-pixel or 150-pixel reference length conditions). This discrepancy between the results and our expectations may be due to the strong positive correlations observed among all conditions (Table 2B, triangle), which may hide the factorial structure underlying the dataset. Also, the strong correlation between both factors and the large difference between the eigenvalues of the two factors suggest that a one-factor model could be an alternative to represent the underlying structure of this dataset.

In Experiment 2, an exploratory factor analysis suggested a four-factor model to best represent the data. The four factors highly loaded on the different conditions that included the horizontal VH, PZ, vertical VH, and ML configurations. This finding corroborates our previous findings, which suggested that there seems to be one factor (or very few factors) per illusion, no matter the specific features of the illusion. Importantly, it seems that there are no proper factors for merged illusions but that merged conditions are well represented by specific combinations of the factors underlying non-merged conditions. Note that we tested more conditions with VH configurations than conditions with ML or PZ configurations. This may explain why two factors related to the VH illusion, while only one factor related to each of the ML and PZ illusion. Similarly, Coren and colleagues (1976) tested several illusions, including 11 variants of the Müller–Lyer illusion and one variant of the Ebbinghaus illusion. They found that two factors highly loaded on the two configurations of the Müller–Lyer variants, while only one factor highly loaded on the two configurations of the Ebbinghaus illusion.

The experimental conditions were different in both experiments. In Experiment 1, the adjustable element was always compared to a reference line, which was not embedded in the context. In contrast, the reference line was always embedded in the context in Experiment 2. As previously suggested, the effect of the vertical–horizontal illusion is weakened when both segments are not in contact (see, for example, Hamburger & Hansen, 2010), which may explain the absence of a factor specifically related to the VH illusion in Experiment 1. In addition, unlike most illusion studies, the illusion stimulus was adjustable but the reference line was fixed in Experiment 1, which may also influence the strength of our results. Indeed, the illusion magnitude varies as a function of the size of the illusion (see, for example, Bulatov, Bertulis, Gutauskas, & Bulatova, 2010).

Contrary to Experiment 1, luminance and noise conditions were better controlled in Experiment 2, and participants were all tested on the same setup. Still, the patterns of results from the path analyses are similar across both experiments; that is, a merged illusion magnitude is strongly predictable from the magnitudes of the two non-merged illusions that made it, suggesting that differences in the experimental designs do not interfere much in the results.

We expected better intrarater reliabilities in Experiment 1 compared to Experiment 2 because there were more repetitions of each condition in Experiment 1 compared to Experiment 2. Nevertheless, intrarater reliabilities were weaker in Experiment 1 ($M = 0.238$, $SD = 0.063$) compared to Experiment 2 ($M = 0.447$, $SD = 0.121$), which may reflect a weakness of the experimental design in Experiment 1 (e.g., lack of

control for external conditions such as noise and other external distractions). Note that the moderate intrarater reliabilities may induce an upper limit on the pairwise correlations, thus leading to underestimated correlations.

In agreement with our previous studies (Cretenoud et al., 2019; Cretenoud et al., 2020), we observed only weak, but mostly positive correlations between different illusions. For example, in Experiment 2, the non-merged ML conditions only weakly correlated with the non-merged PZ conditions ($M = 0.103$, $SD = 0.052$), suggesting that the space underlying visual illusions is multifactorial. However, one-sample two-tailed t-tests on the effect sizes of the between-illusion correlations in both Experiments 1 and 2 were significantly different from zero, suggesting that a small proportion of the variance underlying the illusions is accounted for by a weak common factor.

Contrary to our results, previous studies have often proposed taxonomies for visual illusions. For example, a factor highly loading on the vertical–horizontal, Müller–Lyer, and Ponzo illusions was described as a length factor (Taylor, 1976). However, more specific factors have been sometimes suggested to underlie specific illusions (such as the Müller–Lyer illusion; see Coren et al., 1976). The mixed results may come from discrepancies in the data analysis (e.g., how to determine the number of factors to retain), in the experimental design (e.g., whether or not it is a heterogeneous set of tasks, such that perceptual tasks other than illusions are tested in the same battery), or in the interpretation of the results.

Our research aim was to determine to what extent the magnitudes of the merged illusions can be explained by the magnitudes of the individual illusions and their underlying mechanisms. An extreme case could have been that performance could not be predicted at all—for example, because the merged illusions are not perceived as illusory anymore. Or, one illusion could dominate the other one or there could be some highly nonlinear combinations as often occurs in other fields of cue combination. For example, the joint effects of two grouping cues are sometimes quite different than the sum of the individual effects (e.g., Ben-Av & Sagi, 1995; Huang, 2005; but see Kubovy & Van Den Berg, 2008). Extreme cases are configural superiority effects where small changes in layout strongly change perception (Pomerantz, 2003). However, factors underlying the illusions tested here seem to combine independently.

We like to highlight that the illusion magnitudes of conditions with inward wings were smaller for the 150-pixel compared to the 100-pixel reference line in Experiment 1 (it even changed sign in the case of the vertical adjustable line; see Figure 2). Further investigation is needed to understand this specific pattern of results, which contradicts the general assumption that a task becomes harder when

the stimulus size increases (e.g., see Bulatov et al., 2010).

When the VH illusion was merged with the ML illusion in Experiment 2, we observed stronger path loadings from the VH illusion than from the ML illusion. Similarly, stronger path loadings were observed from the PZ illusion than from the ML illusion when both were merged. The ML illusion therefore seems to have a weaker impact on the merged illusions than the VH and PZ illusions, which may come from the weaker susceptibilities to the ML illusion compared to VH and PZ illusions (see Figure 4 and Table S2B in the Supplementary Material).

In both experiments, the two configurations of an illusion were tested separately. The effects of the two configurations may be additive or superadditive; that is, the illusion magnitude is bigger than the sum of the two individual effects. Foster and Franz (2014) suggested that the Ebbinghaus and Müller–Lyer illusions show superadditive effects when a simultaneous adjustment procedure is used; that is, as the size of one target increases, the size of the other target decreases of a similar amount. On the other hand, they also suggested that there is no superadditivity when an independent adjustment procedure is used; that is, one target is adjustable and the other is the reference (see also Gilster & Kuhtz-Buschbeck, 2010). However, it was shown that the Ebbinghaus illusion magnitude was stronger than the sum of the parts even with an independent adjustment procedure (Grzeczkowski et al., 2018; see also Duemmler, Franz, Jovanovic, & Schwarzer, 2008). Here, we observed asymmetrical illusion magnitudes across both configurations of the same illusion. For example, the inward ML condition yielded stronger illusion magnitudes compared to the outward ML condition in absolute values (Figure 4; see also Cretenoud et al., 2020; Yildiz, Sperandio, Kettle, & Chouinard, 2019). In addition, some illusions showed very weak correlations between the two configurations. For example, the correlation between the inward and outward ML conditions (ML in. and ML out.) in Experiment 2 was not significant ($r = 0.017$, $p = 0.871$). Similarly, we observed strong path loadings between the merged illusions and the non-merged illusions of which they were made, but only in the same configuration. For example, the vertical VH (VH ver.) and the outward ML (ML out.) conditions only weakly loaded on the congruently merged VH-ML illusion when the horizontal segment was adjustable (VH-ML con. hor.). These results suggest that both configurations of an illusion (either merged or non-merged) can have distinct effects at the individual level.

To our knowledge, merged illusions have been tested only once, in a study by Deręgowski (2015), who tested the Ponzo illusion and merged it congruently and incongruently with the Müller–Lyer illusion. There was a significant difference between the effect of the inversion phenomenon on the Ponzo illusion compared to the merged Ponzo/Müller–Lyer illusion, suggesting that the factors underlying the Ponzo and Müller–Lyer illusions have different origins, similarly to what we observed here and has been observed previously (Cretenoud et al., 2019; Grzeczkowski et al., 2017). However, the author did not investigate the relationships between merged and non-merged illusion magnitudes.

To summarize, we previously observed only weak correlations between the susceptibility to different visual illusions but strong correlations between different variants of the same illusion (Cretenoud et al., 2019), suggesting that the structure of the visual space underlying illusions is multifactorial. Here, we investigated whether and how the factors for illusions interact. We tested merged illusions and observed that the susceptibility to a merged illusion is strongly predicted by the susceptibility to the two illusions that made it, suggesting that the factors for illusions combine independently. In comparison with Lavoisier's famous chemistry principle, which claims that nothing is lost, nothing is created but everything is transformed (Lavoisier, 1789), we suggest that in the merged illusions, no factor is lost and no factor is created. Factors are not even transformed—they just combine.

Keywords: illusions, factors, individual differences

References

Aftanas, M. S., & Royce, J. R. (1969). A factor analysis of brain damage tests administered to normal subjects with factor score comparisons across ages. *Multivariate Behavioral Research, 4*(4), 459–481.

Bargary, G., Bosten, J. M., Goodbourn, P. T., Lawrance-Owen, A. J., Hogg, R. E., & Mollon, J. D. (2017). Individual differences in human eye movements: An oculomotor signature? *Vision Research, 141*, 157–169.

Beaujean, A. A. (2014). *Latent variable modeling using R: A step-by-step guide*. London: Routledge.

Ben-Av, M. B., & Sagi, D. (1995). Perceptual grouping by similarity and proximity: Experimental results can be predicted by intensity autocorrelations. *Vision Research, 35*(6), 853–866.

Bosten, J. M., Goodbourn, P. T., Bargary, G., Verhallen, R. J., Lawrance-Owen, A. J., Hogg, R. E., . . . Mollon, J. D. (2017). An exploratory factor analysis of visual performance in a large population. *Vision Research, 141*, 303–316.

Bosten, J. M., & Mollon, J. D. (2010). Is there a general trait of susceptibility to simultaneous contrast? *Vision Research, 50*(17), 1656–1664.

Brainard, D. H. (1997). The Psychophysics Toolbox. *Spatial Vision, 10*(4), 433–436.

Brascamp, J. W., Becker, M. W., & Hambrick, D. Z. (2018). Revisiting individual differences in the time course of binocular rivalry. *Journal of Vision, 18*(7):3, 1–20, https://doi.org/10.1167/18.7.3.

Bulatov, A. (2017). Weight positioned averaging in the illusions of the Müller-Lyer type. In A. G. Shapiro, & D. Todorović (Eds.), *The Oxford compendium of visual illusions* (pp. 159–163). New York: Oxford University Press.

Bulatov, A., Bertulis, A., Gutauskas, A., & Bulatova, N. (2010). Stimulus size and the magnitude of the visual illusion of extent. *Human Physiology, 36*(2), 164–171.

Cao, T., Wang, L., Sun, Z., Engel, S. A., & He, S. (2018). The independent and shared mechanisms of intrinsic brain dynamics: Insights from bistable perception. *Frontiers in Psychology, 9,* 589.

Cappe, C., Clarke, A., Mohr, C., & Herzog, M. H. (2014). Is there a common factor for vision? *Journal of Vision, 14*(8):4, 1–11, https://doi.org/10.1167/14.8.4.

Chamberlain, R., Van der Hallen, R., Huygelier, H., Van de Cruys, S., & Wagemans, J. (2017). Local-global processing bias is not a unitary individual difference in visual processing. *Vision Research, 141*, 247–257.

Cohen, J. (1988). *Statistical power analysis for the behavioral sciences*. Hillsdale, NJ: Lawrence Erlbaum Associates.

Coren, S., Girgus, J. S., Erlichman, H., & Hakstian, A. R. (1976). An empirical taxonomy of visual illusions. *Perception & Psychophysics, 20*(2), 129–137.

Costello, A. B., & Osborne, J. W. (2005). Best practices in exploratory factor analysis: Four recommendations for getting the most from your analysis. *Practical Assessment, Research & Education, 10*(7), 86–99.

Cretenoud, A. F., Grzeczkowski, L., Bertamini, M., & Herzog, M. H. (2020). Individual differences in the Müller-Lyer and Ponzo illusions are stable across different contexts. *Journal of Vision. 20*(6):4, 86–99, https://doi.org/10.1167/jov.20.6.4.

Cretenoud, A. F., Karimpur, H., Grzeczkowski, L., Francis, G., Hamburger, K., & Herzog, M. H. (2019). Factors underlying visual illusions are illusion-specific but not feature-specific. *Journal of Vision, 19*(14):12, 1–21, https://doi.org/https://doi.org/10.1167/19.14.12.

Deręgowski, J. B. (2015). Illusions within an illusion. *Perception, 44*(12), 1416–1421.

Dobkins, K. R., Gunther, K. L., & Peterzell, D. H. (2000). What covariance mechanisms underlie green/red equiluminance, luminance contrast sensitivity and chromatic (green/red) contrast sensitivity? *Vision Research, 40*(6), 613–628.

Duemmler, T., Franz, V. H., Jovanovic, B., & Schwarzer, G. (2008). Effects of the Ebbinghaus illusion on children's perception and grasping. *Experimental Brain Research, 186*(2), 249–260.

Emery, K. J., Volbrecht, V. J., Peterzell, D. H., & Webster, M. A. (2017a). Variations in normal color vision. VI. Factors underlying individual differences in hue scaling and their implications for models of color appearance. *Vision Research, 141*, 51–65.

Emery, K. J., Volbrecht, V. J., Peterzell, D. H., & Webster, M. A. (2017b). Variations in normal color vision. VII. Relationships between color naming and hue scaling. *Vision Research, 141*, 66–75.

Foster, R. M., & Franz, V. H. (2014). Superadditivity of the Ebbinghaus and Müller-Lyer illusions depends on the method of comparison used. *Perception, 43*(8), 783–795.

Frenzel, H., Bohlender, J., Pinsker, K., Wohlleben, B., Tank, J., Lechner, S. G., . . . Lewin, G. R. (2012). A genetic basis for mechanosensory traits in humans. *PLoS Biology, 10*(5), e1001318.

Gignac, G. E., & Szodorai, E. T. (2016). Effect size guidelines for individual differences researchers. *Personality and Individual Differences, 102*, 74–78.

Gilster, R., & Kuhtz-Buschbeck, J. P. (2010). The Müller–Lyer illusion: Investigation of a center of gravity effect on the amplitudes of saccades. *Journal of Vision, 10*(1):11, 1–13, https://doi.org/10.1167/10.1.11.

Grzeczkowski, L., Clarke, A. M., Francis, G., Mast, F. W., & Herzog, M. H. (2017). About individual differences in vision. *Vision Research, 141*, 282–292.

Grzeczkowski, L., Roinishvili, M., Chkonia, E., Brand, A., Mast, F. W., Herzog, M. H., . . . Shaqiri, A. (2018). Is the perception of illusions abnormal in schizophrenia? *Psychiatry Research, 270*, 929–939.

Hamburger, K., & Hansen, T. (2010). Analysis of individual variations in the classical horizontal-vertical illusion. *Attention, Perception & Psychophysics, 72*(4), 1045–1052.

Hibbard, P. B., Bradshaw, M. F., Langley, K., & Rogers, B. J. (2002). The stereoscopic anisotropy: Individual differences and underlying mechanisms. *Journal of Experimental Psychology: Human Perception and Performance, 28*(2), 469–476.

Huang, L. (2005). Grouping by similarity is mediated by feature selection: Evidence from the failure of cue combination. *Psychonomic Bulletin & Review, 22*(5), 1364–1369.

Iglewicz, B., & Hoaglin, D. (1993). *Volume 16: How to detect and handle outliers*. Milwaukee, WI: ASQC Press.

John, O. P., & Srivastava, S. (1999). The Big Five trait taxonomy: History, measurement, and theoretical perspectives. In L. A. Pervin, & O. P. John (Eds.), *Handbook of personality: Theory and research* (Vol. *2*, pp. 102–138). New York: Guilford Press.

Koo, T. K., & Li, M. Y. (2016). A guideline of selecting and reporting intraclass correlation coefficients for reliability research. *Journal of Chiropractic Medicine, 15*(2), 155–163.

Kubovy, M., & Van Den Berg, M. (2008). The whole is equal to the sum of its parts: A probabilistic model of grouping by proximity and similarity in regular patterns. *Psychological Review, 115*(1), 131–154.

Lavoisier, A. L. (1789). *Traité élémentaire de chimie (Elementary Treatise on Chemistry)*. Paris: Cuchet.

Milne, E., & Szczerbinski, M. (2009). Global and local perceptual style, field-independence, and central coherence: An attempt at concept validation. *Advances in Cognitive Psychology, 5*, 1–26.

Mollon, J. D., Bosten, J. M., Peterzell, D. H., & Webster, M. A. (2017). Individual differences in visual science: What can be learned and what is good experimental practice? *Vision Research, 141*, 4–15.

Pelli, D. G. (1997). The VideoToolbox software for visual psychophysics: Transforming numbers into movies. *Spatial Vision, 10*(4), 437–442.

Peterzell, D. H. (2016). Discovering sensory processes using individual differences: A review and factor analytic manifesto. *Electronic Imaging*, 2016(*16*), 1–11.

Peterzell, D. H., Chang, S. K., & Teller, D. Y. (2000). Spatial frequency tuned covariance channels for red-green and luminance-modulated gratings: Psychophysical data from human infants. *Vision Research, 40*(4), 431–444.

Peterzell, D. H., Schefrin, B. E., Tregear, S. J., & Werner, J. S. (2000). Spatial frequency tuned covariance channels underlying scotopic contrast sensitivity. In: *Vision science and its applications*, OSA Technical Digest, paper FC2. Washington, D.C.: Optical Society of America.

Peterzell, D. H., Serrano-Pedraza, I., Widdall, M., & Read, J. C. A. (2017). Thresholds for sine-wave corrugations defined by binocular disparity in random dot stereograms: Factor analysis of individual differences reveals two stereoscopic mechanisms tuned for spatial frequency. *Vision Research, 141*, 127–135.

Pomerantz, J. R. (2003). Wholes, holes, and basic features in vision. *Trends in Cognitive Sciences, 7*(11), 471–473.

Preacher, K. J., Zhang, G., Kim, C., & Mels, G. (2013). Choosing the optimal number of factors in exploratory factor analysis: a model selection perspective. *Multivariate Behavioral Research, 48*(1), 28–56.

R Core Team. (2018). The R project for statistical computing. Retrieved from https://www.r-project.org/.

Robinson, J. O. (1968). Retinal inhibition in visual distortion. *British Journal of Psychology, 59*(1), 29–36.

Roff, M. (1953). *A factorial study of tests in the perceptual area* (pp. 1–41), Psychometric Monographs 8. Madison, WI: Psychometric Society.

Shrout, P. E., & Fleiss, J. L. (1979). Intraclass correlations: uses in assessing rater reliability. *Psychological Bulletin, 86*(2), 420–428.

Taylor, T. R. (1974). A factor analysis of 21 illusions: The implications for theory. *Psychologia Africana, 15*, 137–148.

Taylor, T. R. (1976). The factor structure of geometric illusions: A second study. *Psychologia Africana, 16*, 177–200.

Thurstone, L. L. (1944). *A factorial study of perception*. Chicago, IL: The University of Chicago Press.

Tulver, K. (2019). The factorial structure of individual differences in visual perception. *Consciousness and Cognition, 73*, 102762.

Tulver, K., Aru, J., Rutiku, R., & Bachmann, T. (2019). Individual differences in the effects of priors on perception: A multi-paradigm approach. *Cognition, 187*(3), 167–177.

Verhallen, R. J., Bosten, J. M., Goodbourn, P. T., Lawrance-Owen, A. J., Bargary, G., & Mollon,

J. D. (2017). General and specific factors in the processing of faces. *Vision Research, 141*, 217–227.

Webster, M. A., & MacLeod, D. I. A. (1988). Factors underlying individual differences in the color matches of normal observers. *Journal of the Optical Society of America, 5*(10), 1722–1735.

Wechsler, D. (2003). *Wechsler intelligence scale for children* (4th ed.). San Antonio, TX: The Psychological Corporation.

Yildiz, G. Y., Sperandio, I., Kettle, C., & Chouinard, P. A. (2019). The contribution of linear perspective cues and texture gradients in the perceptual rescaling of stimuli inside a Ponzo illusion corridor. *PLoS One, 14*(10), e0223583.